Epoxidation of light olefin mixtures with hydrogen peroxide on TS-1 in a laboratory-scale trickle bed reactor

Alvear, Matias; Orabona, Federica; Eränen, Kari; Lehtonen, Juha; Rautiainen, Sari; Di Serio, Martino; Russo, Vincenzo; Salmi, Tapio

Published in:
Chemical Engineering Science

DOI:
10.1016/j.ces.2023.118467

Published: 05/04/2023

Document Version
Final published version

Document License
CC BY

Chemical Engineering Science 269 (2023) 118467

Contents lists available at ScienceDirect

Chemical Engineering Science

journal homepage: www.elsevier.com/locate/ces

Epoxidation of light olefin mixtures with hydrogen peroxide on TS-1 in a laboratory-scale trickle bed reactor: Transient experimental study and mathematical modelling

Matias Alvear [a], Federica Orabona [a,b], Kari Eränen [a], Juha Lehtonen [a,c], Sari Rautiainen [c], Martino Di Serio [b], Vincenzo Russo [a,b], Tapio Salmi [a,*]

[a] Åbo Akademi, Laboratory of Industrial Chemistry and Reaction Engineering (TKR), FI-20500 Turku/Åbo, Finland
[b] Università degli Studi di Napoli 'Federico II', Department of Chemical Sciences, IT-80126 Napoli, Italy
[c] VTT Technical Research Centre of Finland Ltd, P.O. Box 1000, FI-02044 VTT Espoo, Finland

HIGHLIGHTS

- Ethene, propene and 1-butene mixtures were selectively epoxidized with H_2O_2 on TS-1 as heterogeneous catalyst.
- The epoxidation of different olefins took place simultaneously.
- Extensive transient and stationary experiments were conducted in a trickle bed reactor (TBR).
- A trickle bed model was employed to describe the experimental data.

ARTICLE INFO

Article history:
Received 24 November 2022
Received in revised form 29 December 2022
Accepted 7 January 2023
Available online 9 January 2023

Keywords:
Epoxidation
Olefin mixtures
Trickle bed reactor
Kinetic modeling
Reactor modelling

ABSTRACT

Direct epoxidation of light olefin mixtures with hydrogen peroxide and titanium silicalite (TS-1) catalyst is interesting from a pure scientific viewpoint and it might have a considerable economic and environmental advantages. Direct epoxidation of olefin mixtures implies a significant process intensification as the separation steps of alkenes prior to the epoxidation process is avoided. Binary and ternary mixtures of ethene, propene and 1-butene were selectively epoxidized with hydrogen peroxide in the presence of TS-1 as the heterogeneous catalyst. Methanol was used as the solvent. Transient and stationary kinetic experiments were conducted in a laboratory-scale trickle bed reactor, which was operated under atmospheric pressure and isothermal conditions at 15–55 °C. The experiments were designed to investigate the kinetics of the epoxidation of light olefins at different temperatures, alkene-to-hydrogen peroxide molar ratios as well as gas and liquid residence times in the trickle bed reactor. The recorded transient responses of the reaction products confirmed that the components in the alkene mixtures are epoxidized simultaneously. The epoxide selectivity was 90 % or higher in most experiments; ring-opening products formed from the epoxides and methanol were observed as by-products. The concentration maxima of epoxides during the transient experiments were explained by accumulation of the epoxide products inside the catalyst, which resulted in partial blocking of active sites. After-treatment of the catalyst with methanol and nitrogen completely restored the initial activity. Kinetic modeling was applied, based on presumed elementary steps on the TS-1 surface to describe the behavior of the system at steady state conditions. The trickle bed reactor was described with a dynamic multiphase model, taking into account the kinetic and mass transfer effects. The numerical values of the activation energies, kinetic constants and mass transfer parameters were estimated by nonlinear regression analysis. The model gave a satisfactory description of the experimental data.

1. Introduction

Ethene oxide, propene oxide and 1-butene oxide are highly reactive chemicals used as raw materials for the manufacture of polyether polyols, glycols, and glycol ethers (Smith, 1984; Berndt

* Corresponding author.

https://doi.org/10.1016/j.ces.2023.118467
0009-2509/

Nomenclature

a_{GL}	Gas-liquid interfacial area [m^{-1}]
a_{LS}	Liquid-solid interfacial area [m^{-1}]
$C_{i,G}$	Concentration of species *i* in the gas phase G [mol/m^3]
$C_{i,L}$	Concentration of species *i* in the liquid phase L [mol/m^3]
$D_{A,B}$	Molecular diffusivity of olefin A in the liquid phase B [m^2/min]
D_i	Reactor internal diameter [cm]
d_k	Krischer-Kast hydraulic diameter [m]
d_p	Particle diameter [μm]
Ea	Activation energy [kJ/mol]
H	Henry's constant [-]
k	Kinetic constant
k_0	Reference kinetic constant calculated at T_{ref}
K_{ads}	Adsorption constant [-]
k_g	Gas-phase mass transfer coefficient [m/min]
k_L	Liquid-phase mass transfer coefficient [m/min]
L	Reactor length [cm]
M	Molecular mass [g/mol]
N_{GL}	Gas-liquid flux [$mol/(m^2\ min)$]
P	Pressure [bar]
Pe_G	Péclet number for gas phase [-]
Pe_L	Péclet number for liquid phase [-]
Re_L	Reynolds number for liquid phase [-]
R_G	Ideal gas constant [kJ/(K mol)]
R	Reaction rate [$mol/(kg_{cat}\ min)$]
Sc_L	Schmidt number for liquid phase
T	Temperature [K]
t	Time [min]
T_{ref}	Reference temperature [K]
u_G	Gas-phase superficial velocity [m/min]
u_L	Liquid-phase superficial velocity [m/min]
V_A	Molar volume of the solute A at its normal boiling point [m^3/mol]
We_L	Weber number for liquid phase [-]
X_G	Modified Lockhart-Martinelli ratio [-]

Greek letters

α	Wetting efficiency parameter [mL/min]
β	Wetting efficiency parameter [-]
ε_B	Bed porosity [-]
ε_G	Gas-phase hold up [-]
ε_L	Liquid-phase hold up [-]
ε_S	Solid-phase hold up [-]
η_{LS}	Wetting efficiency [-]
μ_L	Liquid-phase viscosity [Pa s]
$\nu_{i,j}$	Stoichiometric coefficient for component *i* in reaction *j* [–]
ρ_b	Catalyst bulk density referred to liquid phase [kg/m^3]
ρ_s	Solid density [kg/m^3]
χ	Dimensionless axial coordinate [-]
σ_L	Liquid surface tension [N/m]
ϕ	Association factor of solvent [-]

Abbreviations

G	Gas
GFR	Gas flow rate
L	Liquid
LFR	Liquid flow rate
TOS	Time-on-stream
*	Surface site

and Bräsel, 2009; Grigoropoulou et al., 2003). Two main synthesis routes of industrial scale have been developed for the production of propene oxide: chlorohydrin route and alkene epoxidation route, which are multiphase (gas–liquid-solid catalyst) processes. However, since a huge amounts of chlorine by-products are obtained in the first process and global environmental awareness requires cleaner technologies, scientific research has been focused on studying direct epoxidation of alkenes (Jess and Wasserscheid, 2013). For the industrial production of ethene oxide, gas-phase epoxidation is applied on promoted silver catalysts. Lefort (1935) discovered that metallic silver can catalyze the reaction between molecular oxygen and ethene to produce ethene oxide at 250–300 °C. However, silver catalyst is not efficient in direct oxidation of alkenes with allylic hydrogens, such as propene and 1-butene (Rebsdat and Mayer, 2000).

In 1983, the Italian enterprise ENI patented the first catalyst for direct epoxidation of propene with hydrogen peroxide, titanium silicalite-1 (TS-1) (Taramasso et al., 1983; Russo et al., 2013; Clerici et al., 1991). Hydrogen peroxide has the great benefit as it makes the process economically and environmentally friendly, since only water is produced as the stoichiometric co-product under mild conditions, i.e. at moderate temperatures and pressures (Speight, 2011). The active site on TS-1 is considered to the closed $Ti(OSi)_4$ tetrahedral site which interacts with hydrogen peroxide and the solvent, forming an operative site being able to capture the olefin and form the epoxide. TS-1 shows outstanding catalytic performance not only in the epoxidation of propene but also of other linear short-chained alkenes (Notari, 1996; Clerici and Ingallina, 1993), which gives the opportunity to epoxidize olefin mixtures with a single catalyst, and avoiding separation steps of alkenes prior to the epoxidation step. In currently operating ethene plants, ethene, propene and butenes are separated before further treatment. However, a way to utilize biomass is to convert it to synthesis gas consisting mainly of carbon monoxide and hydrogen. By applying the Fischer-Tropsch concept on the synthesis gas, a mixture of alkenes is obtained and it is attractive to study the behavior of alkene mixtures.

We have in our previous research investigated the epoxidation of individual alkenes (Alvear et al., 2021a, 2021b, 2022). In this work, binary and tertiary mixtures of ethene, propene and 1-butene were selectively epoxidized with hydrogen peroxide and TS-1 as the heterogeneous catalyst in a laboratory-scale trickle bed reactor operating under transient and stationary conditions. The experimental landscape was a three-phase system with a complex reaction scheme that had not been investigated in previous literature. The behavior of the epoxidation of olefin mixtures was studied to obtain reliable kinetic information related to the surface reaction steps. A kinetic model was developed to describe the behavior of the system under stationary conditions.

2. Experimental section

2.1. Chemicals

The gases were nitrogen (AGA), ethene (AGA), propene (AGA), and 1-butene (Linde). Aqueous solutions of hydrogen peroxide (>30 wt%, Fisher Chemicals), highly pure methanol (>99.9 wt%, Sigma Aldrich), 1-methoxyethanol (>99.5 wt%, Sigma Aldrich),

ethylene glycol (>99.5 wt%, Fluka), propylene glycol (<99.5%, Sigma Aldrich), propylene oxide (99.9%, Sigma Aldrich, 1-methoxy-2-propanol (>99.5%, Sigma-Aldrich), 1,2-epoxybutane (99%, Sigma Aldrich), 1-methoxy-2-butanol (97%, Sigma Aldrich), 1,2-butanediol (>98%, Sigma Aldrich), ferroin indicator (0.1wt%, Sigma Aldrich), cerium sulphate solution (0.1 M, honeywell) were used without further purification. Commercial titanium-silicalite (TS-1) of ACS material type B was employed as the heterogeneous catalyst: CAS No 13463-67-7 (titanium dioxide)/7621-86-9 (silicon dioxide).

2.2. Experimental equipment and procedures

The kinetic experiments were carried out in the experimental set-up illustrated in the flowsheet in Fig. 1.

The gas phase comprising nitrogen, ethene, propene and 1-butene was fed into the trickle bed reactor through Brook Instruments mass flow controllers (MFC-1, MFC-2, MFC-3 and MFC-4). Simultaneously, a solution of H_2O_2 in methanol was pumped into the reactor through an Agilent 1100 Series HPLC pump. The mass flow of the solution of H_2O_2 in methanol was checked by an analytical balance. Typical mole fractions in the liquid feed were 0.892 for methanol, 0.076 for water and 0.032 for hydrogen peroxide. The trickle bed reactor had an internal diameter of 1.5 cm and a length of 34 cm. Inside the reactor, the catalyst bed was made up of 1 g of TS-1 mixed with 20 g of quartz beads. The remaining volume of the reactor was filled with quartz sand to get a better distribution and mixing of the reactants through the bed. To reach good thermal control, the reactor was completely covered by a heating coil in which water from a thermostatic bath was circulating. The pressure of the system was controlled by Equilibar U3L Ultra Low Flow Back Pressure Regulator (PC-1), assuring that the liquid phase could not return back to the reactor but passed to the 50 mL gas–liquid separator. The gas phase flowed through a condenser at 15 °C, and then analyzed online by a Micro Gas Chromatograph (Agilent 490 Micro GC) equipped with a micro thermal conductivity detector (TCD). At the same time, liquid samples were collected from the bottom of the liquid–gas separator and analyzed offline via a GC (Agilent 6890N) equipped with a TCD. The conditions of trickle flow in the reactor system were checked before the experiments. The ratios between the liquid and gas densities and velocities were calculated and based on flow charts for three-phase fixed beds (Alvear et al., 2021a; Salmi et al., 2019). It was confirmed that the reactor operated under trickle flow conditions.

2.3. Kinetic experiments

Kinetic experiments on the epoxidation of 1-butene-propene binary mixture (Table 1) and 1-butene-propene-ethene ternary mixture (Table 2) were carried out by applying transient techniques, i.e. step response experiments. The liquid flow, the reaction temperature and hydrogen peroxide concentration were varied to study the effect of these parameters on the reaction kinetics and product distribution. The upper temperature was limited to 55 °C, because hydrogen peroxide decomposition starts to increase above this temperature.

3. Experimental results and discussion

3.1. Epoxidation of 1-butene-propene binary mixtures

3.1.1. Temperature effect

The effect of the reaction temperature on propene and 1-butene conversions and product selectivities are displayed in Figs. 2–3, respectively. Propene oxide (PO) and 1-butene oxide (BO) where always the main products, whereas 2-methoxypropanol and 2-methoxybutanol were the secondary products formed via ring opening caused by methanol. By increasing the reaction temperature, both propene and 1-butene conversions were considerably enhanced, and the dynamics of the step responses became faster, but kept similar forms. The step responses of the main products, the epoxides are very similar, thus indicating that they are formed in parallel, in analogous surface reaction steps. A maximum of the epoxide concentration was observed in most experiments. In case of competitive adsorption of reactants, such a maximum in the product concentration is expected, if some of the reactants or products have clearly stronger adsorption affinity and start to dominate on the surface at steady state. The catalyst was post-treated after the experiment with inert gas (N_2) and methanol at elevated temperature (80 °C) and pressure (4 bar) and reaction products were

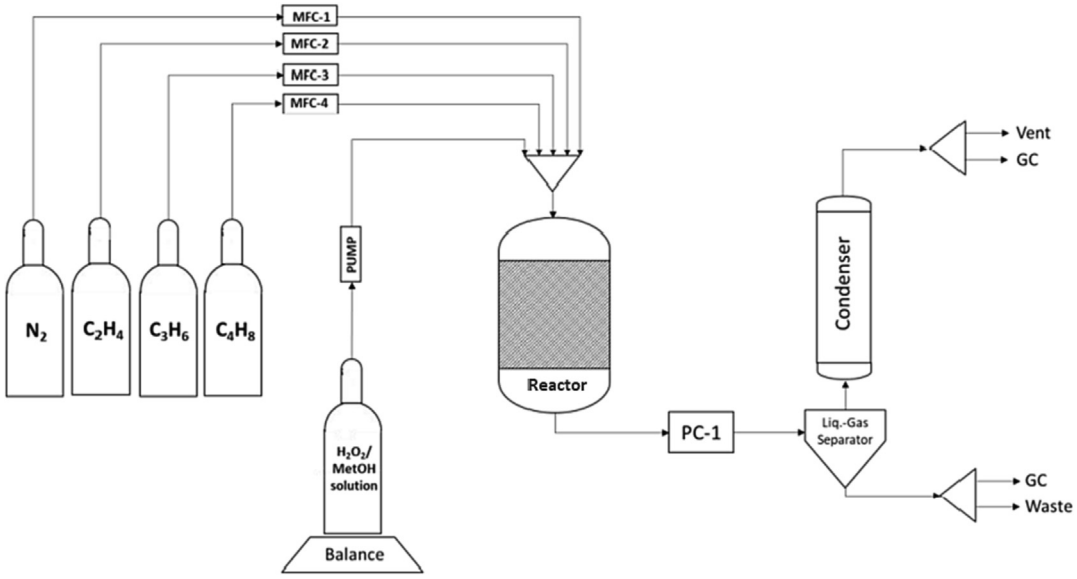

Fig. 1. Experimental set-up for epoxidation of alkene mixtures.

Table 1
Experimental matrix for epoxidation of 1-butene-propene mixtures.

Experiment	T [°C]	P [bar]	Gas flow [mmol/min]			Liquid flow	H_2O_2 wt%
			Propene	1-Butene	N_2	[mL/min]	
T1	55	1	0.112	0.112	0.223	0.5	2
T2	45	1	0.112	0.112	0.223	0.5	2
T3	15	1	0.112	0.112	0.223	0.5	2
L1	45	1	0.112	0.112	0.223	1	2
L2	45	1	0.112	0.112	0.223	2	2
H1	45	1	0.112	0.112	0.223	0.5	1
H2	45	1	0.112	0.112	0.223	0.5	4
G1	45	1	0.223	0.112	0.112	0.5	2
G2	45	1	0.112	0.223	0.112	0.5	2

wt% H_2O_2 in the liquid feed consisting of methanol, H_2O and H_2O_2.

Table 2
Experimental matrix for epoxidation of ethene-propene-1-butene mixtures.

Experiment	T	P	Gas flow				Liquid flow	H_2O_2
	°C	bar	mmol/min				mL/min	wt%
			Ethene	Propene	1-Butene	Nitrogen		
T1	55	1	0.112	0.112	0.112	0.112	0.5	2
T2	45	1	0.112	0.112	0.112	0.112	0.5	2
T3	35	1	0.112	0.112	0.112	0.112	0.5	2
T4	25	1	0.112	0.112	0.112	0.112	0.5	2
T5	15	1	0.112	0.112	0.112	0.112	0.5	2
L1	45	1	0.112	0.112	0.112	0.112	0.75	2
L2	45	1	0.112	0.112	0.112	0.112	1	2
L3	45	1	0.112	0.112	0.112	0.112	1.5	2
L4	45	1	0.112	0.112	0.112	0.112	2	2
H1	45	1	0.112	0.112	0.112	0.112	0.5	1
H2	45	1	0.112	0.112	0.112	0.112	0.5	1.5
H3	45	1	0.112	0.112	0.112	0.112	0.5	3
H4	45	1	0.112	0.112	0.112	0.112	0.5	4

wt% H_2O_2 in the liquid feed consisting of methanol, H_2O and H_2O_2.

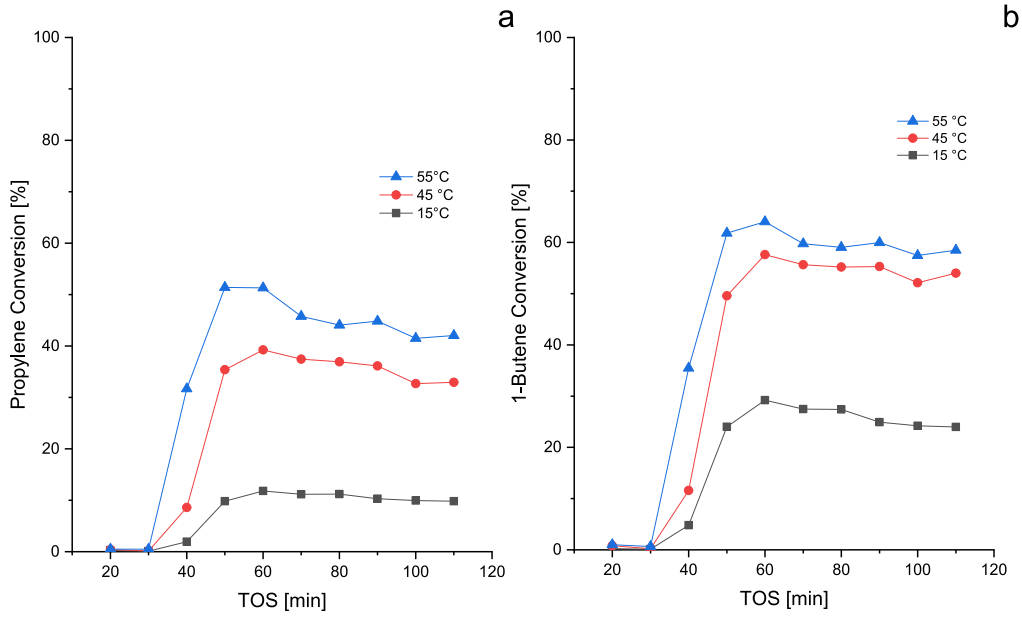

Fig. 2. Effect of the reaction temperature on propene conversion (a) and 1-butene conversion (b). Reaction conditions: P = 1 bar; LFR = 0.5 mL/min; GFR = 0.446 mmol/min; wt % H_2O_2 = 2.

released from the catalyst as confirmed by gas chromatography. After this treatment, the catalyst activity was completely restored.

Ring opening reactions of PO and BO to 2-methoxypropanol and 2-methoxybutanol were not detected at 15 °C but they became relevant at 45 and 55 °C. After the initiation period, the propene oxide (PO) and 1-butene oxide (BO) selectivities remained on constant levels, but diminished with temperature, from 100 % at 15 °C to approximately 90 % at 55 °C. As the main and side reactions are

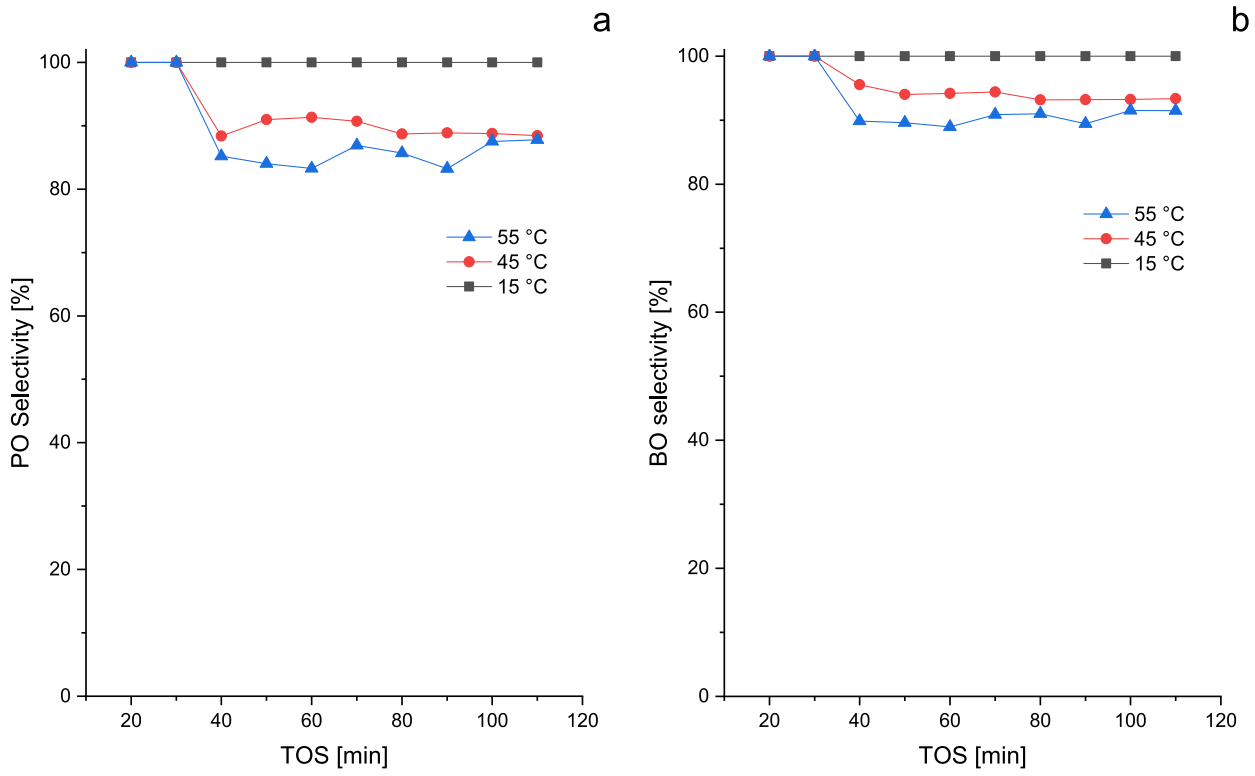

Fig. 3. Effect of reaction temperature on propene oxide selectivity (a) and 1-butene oxide selectivity (b). Reaction conditions: P = 1 bar; LFR = 0.5 mL/min; GFR = 0.446 mmol/min; wt% H_2O_2 = 2.

irreversible and consecutive, the selectivity to the desired product decreases, while that of the undesired product increases with conversion. The increase of the by-product formation with increasing temperature indicates that the activation energies of the ring opening reactions are higher than the activation energies of epoxidation. At 55 °C the hydrogen peroxide decomposition becomes important as has been reported in our previous work (Alvear et al., 2021a, 2021b); therefore the highest experimental temperature was fixed at 55 °C. No oxidation products of methanol were detected, as confirmed by the gas chromatographic analysis. Methanol is known to be a good solvent for alkene epoxidation because it is not oxidized by hydrogen peroxide under mild reaction conditions.

3.1.2. Effect of liquid flow rate

The liquid flow rate was varied to study how the residence time affects the olefin conversion and the epoxide selectivity. The transient responses are displayed in Figs. 4 and 5. Also here both olefins showed a very similar behavior. Both propene and 1-butene conversions dropped by increasing the liquid flow rate from 0.5 mL/min to 2 mL/min, due to a shorter residence time of the reactants in the reactor. Simultaneously, the PO and BO selectivities were positively influenced by an increase of the volumetric flow rate. The consecutive reactions to 2-methoxypropanol and 2-methoxybutanol were suppressed with increasing the flow rates, giving 100 % of selectivity to PO and BO at 2 mL/min.

3.1.3. Effect of hydrogen peroxide concentration

The effect of the hydrogen peroxide concentration on olefin conversions and epoxide selectivities was investigated by varying the concentration of H_2O_2. The results are displayed in Figs. 6 and 7. By increasing the hydrogen peroxide concentration from 1 to 2 wt%, the propene and 1-butene conversions were improved. However, a further increase of the hydrogen peroxide concentration to 4 wt% did not anymore affect the conversions. A possible explanation can be the adsorption effect: it is known that the adsorbed complex of hydrogen peroxide on TS-1 plays a key role in the reaction mechanism, thus a saturation coverage on the catalyst surface is approached as the peroxide concentration is increased. Concerning the product distribution, the effect of the peroxide concentration on the PO and BO selectivities is minor, as illustrated in Fig. 7.

3.1.4. Effect of gas composition

The effect of the gas composition on the propene and 1-butene conversions as well as on epoxide selectivities was investigated by varying the propene-to-1-butene molar ratio, while maintaining the total gas flow rate constant.

An experiment was carried out with a 2:1 propene-to-1-butene molar ratio, in which the propene flow was doubled. The results are displayed in Figs. 8 and 9. Compared to the equimolar experiment, both olefin conversions decreased, while the PO and BO selectivities did not change. The other experiment was dual to the first, with a 1:2 C_3H_6-to-C_4H_8 molar ratio as shown in Figs. 10 and 11. Similarly, the propene and 1-butene conversions decreased but the epoxide selectivities were practically the same by shifting the molar ratio from equimolar conditions.

3.2. Epoxidation of 1-butene-propene-ethene ternary mixture

3.2.1. Temperature effect

The conversions of ethene, propene and 1-butene are shown in Fig. 12, while the epoxide selectivities are displayed in Fig. 13. Similarly to the binary mixture, the propene, 1-butene and ethene conversions were improved by increasing the reaction temperature. At the same time, the PO and BO selectivities remained stable at 100 % from 15 to 35 °C, but decreased to approximately 90 % from 45 to 55 °C. For EO, a 100 % selectivity was detected in all the experi-

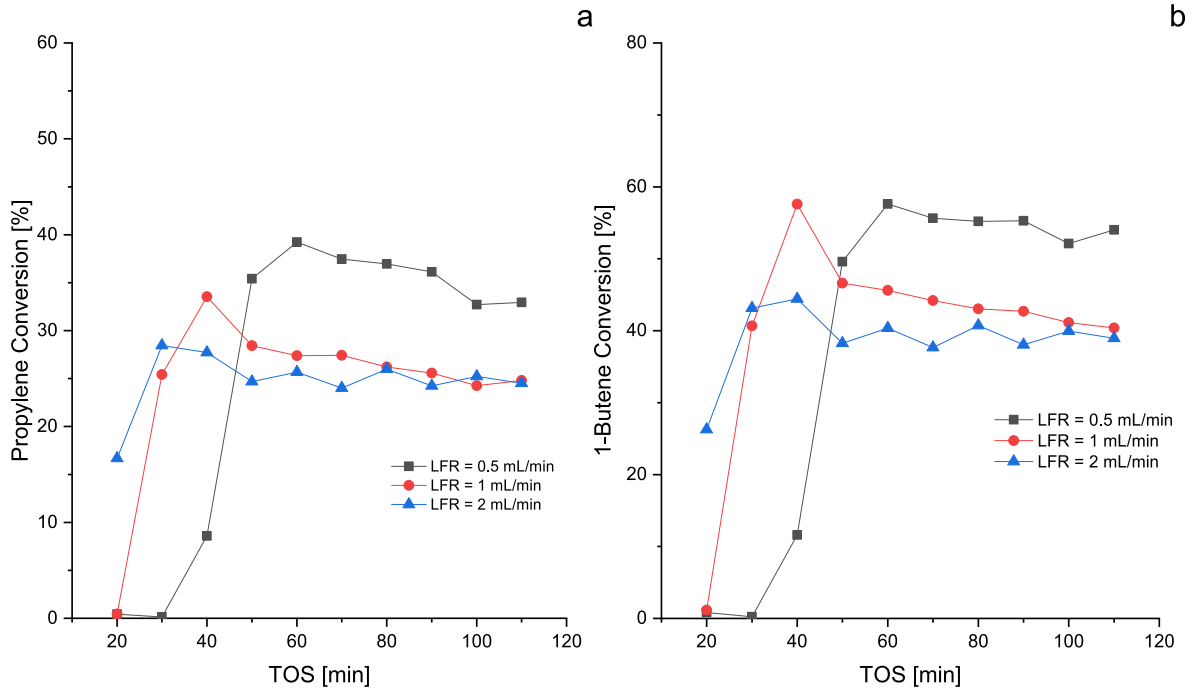

Fig. 4. Effect of liquid flow rate (LFR) on propene conversion (a) and 1-butene conversion (b). Reaction conditions: T = 45 °C; P = 1 bar; GFR = 0.446 mmol/min; wt% H_2O_2 = 2.

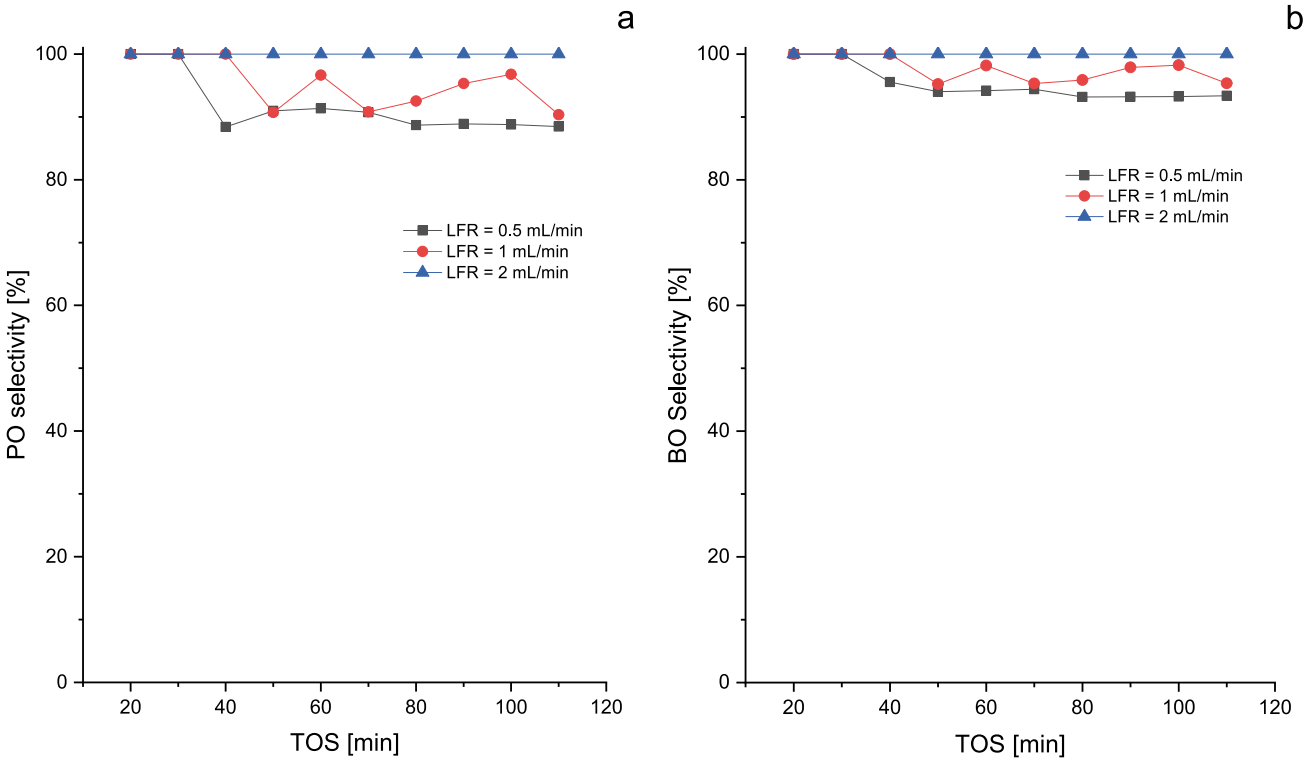

Fig. 5. Effect of liquid flow rate (LFR) on propene oxide selectivity (a) and 1-butene oxide selectivity (b). Reaction conditions: T = 45 °C; P = 1 bar; GFR = 0.446 mmol/min; wt% H_2O_2 = 2.

ments. The transient behaviors of the epoxides showed an interesting behavior: the step response of ethene oxide was monotonic, whereas a maximum was noticed for the PO and BO responses. This can be due to the presence of BO side products in the pores affecting the accessible titanium active sites for butene epoxidation.

3.2.2. Effect of liquid flow rate

Compared to propene-1-butene system, the ternary mixture showed a more complex behavior as the liquid flow rate was increased. Although a reduction of the residence time was expected to affect negatively the olefin conversions, they did not remarkably change, as shown in Fig. 14. In addition, the pro-

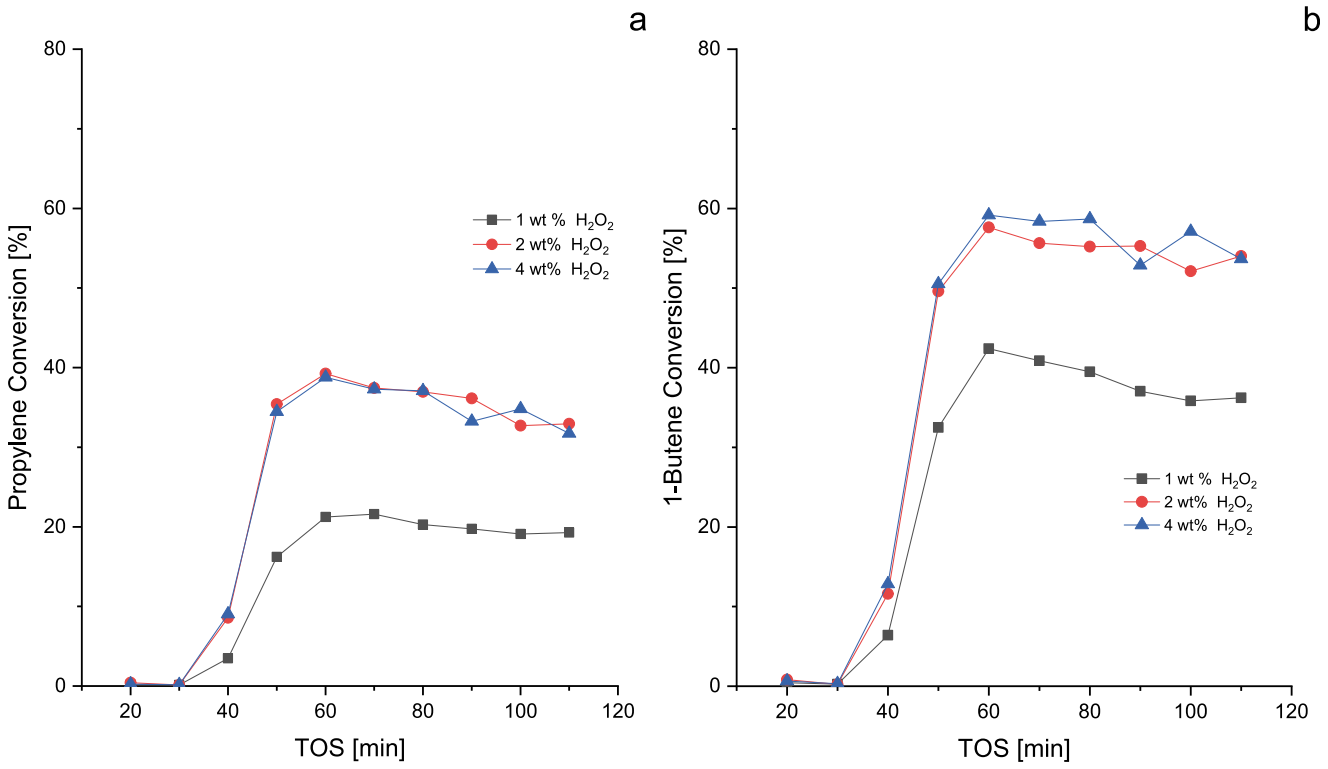

Fig. 6. Effect of H_2O_2 concentration on propene conversion (a) and 1-butene conversion (b). Reaction conditions: T = 45 °C; P = 1 bar; LFR = 0.5 mL/min; GFR = 0.446 mmol/min.

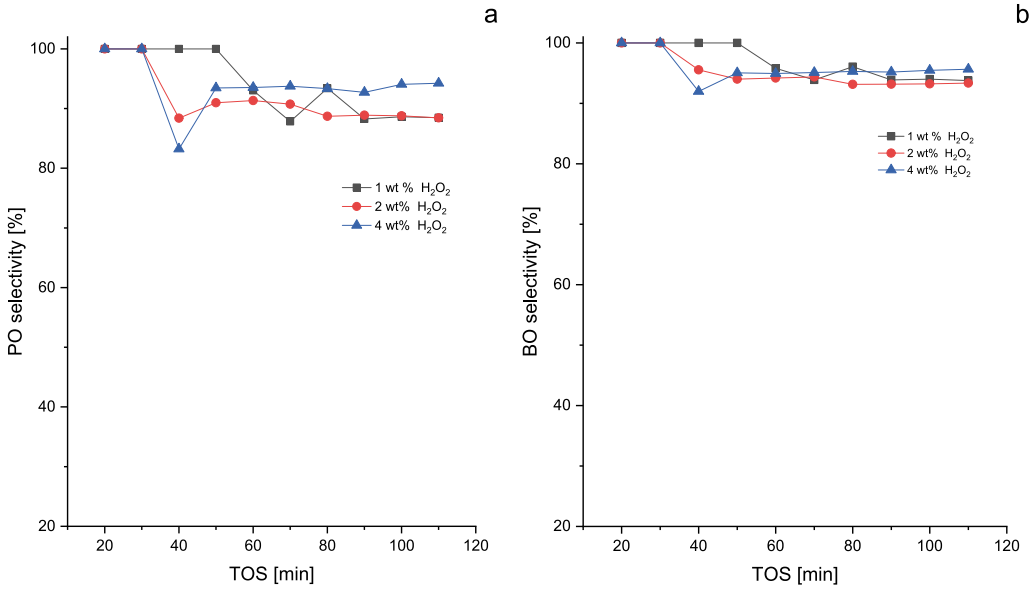

Fig. 7. Effect of H_2O_2 concentration on propene oxide selectivity (a) and 1-butene oxide selectivity (b). Reaction conditions: T = 45 °C; P = 1 bar; LFR = 0.5 mL/min; GFR = 0.446 mmol/min.

pene and 1-butene conversions showed a maximum at the flowrate 1.5 mL/min, while the ethene conversion had a maximum at at 1 mL/min. A competition between two effects needs to be taken into account: the effect of the residence time and the external mass transfer around the catalyst particles. Until the flow rate 1.5 mL/min, the reduction in the residence time is balanced by the increase of the liquid–solid mass transfer coefficient, which depends on the liquid flowrate. As the flowrate is further increased, the decrease of the residence time begins to have a dominating effect and the conversion decreases. Fig. 15 shows that the epoxide selectivities were stable and very high in all the cases.

3.2.3. *Effect of hydrogen peroxide concentration*

The hydrogen peroxide concentration was varied to reveal its effect on the ethene, propene and 1-butene conversions as well

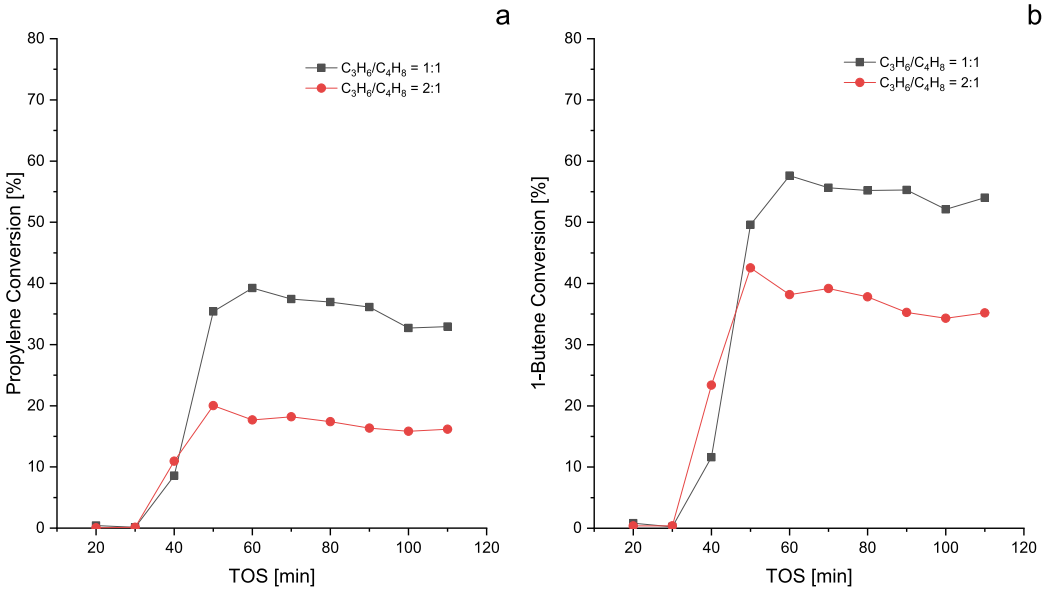

Fig. 8. Effect of gas composition on propene conversion (a) and 1-butene conversion (b). Reaction conditions: T = 45 °C; P = 1 bar; LFR = 0.5 mL/min; GFR = 0.446 mmol/min; wt% H_2O_2 = 2.

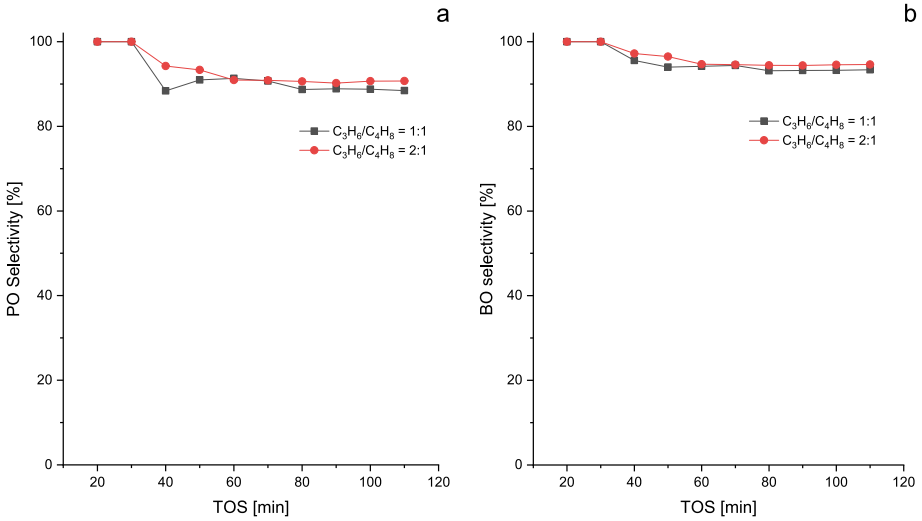

Fig. 9. Effect of gas composition on propene oxide selectivity (a) and 1-butene oxide selectivity (b). Reaction conditions: T = 45 °C; P = 1 bar; LFR = 0.5 mL/min; GFR = 0.446 mmol/min; wt% H_2O_2 = 2.

as on the epoxide selectivities. As illustrated in Fig. 16, the conversions increased by concentrating the liquid phase from 1 to 3 wt% of hydrogen peroxide in methanol, but the selectivities to ethene oxide, propene oxide and 1-butene oxide were approximately 100 %, not being affected by a variation of the hydrogen peroxide concentration as can be seen in Fig. 17.

3.3. Reaction scheme

The reaction scheme is displayed in Fig. 18. Under the investigated range of experimental conditions, 1-methoxy-2-propanol and 1-methoxy-2-butanol were the only by-products formed, while no glycols were observed.

In the present case, the impact of the side reactions, the ring opening reactions was minor, because the epoxide selectivity typically exceeded 90 %.

3.4. The role of active sites on TS-1 and the effect of alkene chain length on conversion

In all the experiments, the olefin conversion was observed to decrease in the order 1-butene > propene > ethene. The issues which have to be addressed when discussing the reactivities of alkenes are the steric hindrance, the alkene solubility in methanol and the inductive effect. In general, steric hindrance plays a crucial role in olefin reactivity when microporous crystalline TS-1 is employed as the catalyst (Grigoropolou et al., 2005; Clerici, 2015). As a matter of fact, the smaller and more linear are the molecules, the faster they diffuse in the catalyst micropores. However, this would not describe the observed reactivity order, if considered as the main and single effect. In all the experiments, 1-butene was indeed the biggest and the most reactive olefin, implying that other effects are predominant. As the epoxidation reaction occurs in liquid phase, the olefin solubilities in methanol strongly

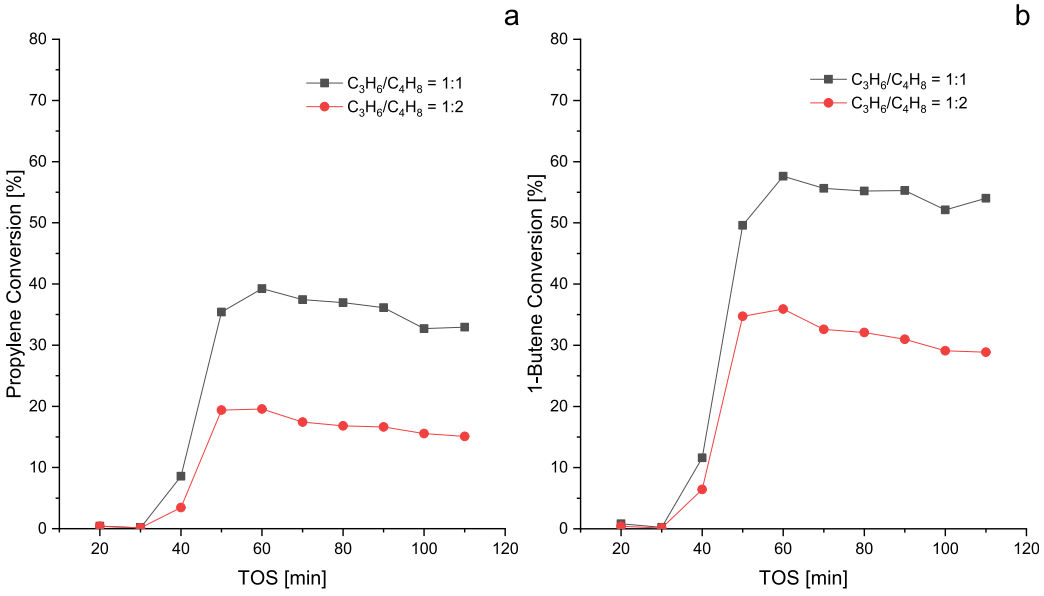

Fig. 10. Effect of gas composition on propene conversion (a) and 1-butene conversion (b). Reaction conditions: T = 45 °C; P = 1 bar; LFR = 0.5 mL/min; GFR = 0.446 mmol/min; wt% H_2O_2 = 2.

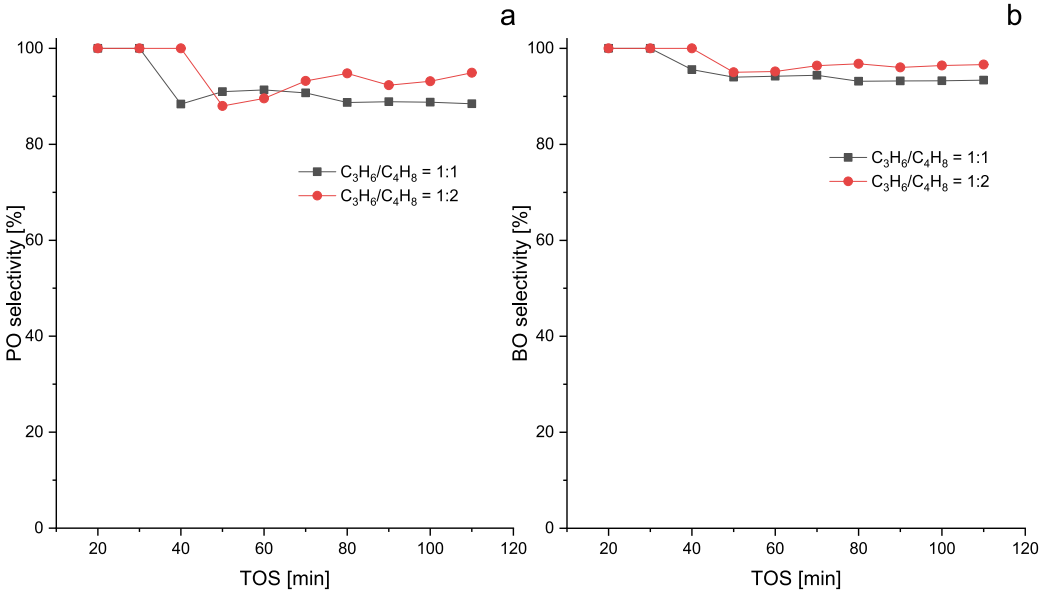

Fig. 11. Effect of gas composition on propene oxide selectivity (a) and 1-butene oxide selectivity (b). Reaction conditions: T = 45 °C; P = 1 bar; LFR = 0.5 mL/min; GFR = 0.446 mmol/min; wt% H_2O_2 = 2.

affect their reactivities. Table 3 (Section 4.3) reveals that the gas solubilities follow the order 1-butene > propene > ethene. Furthermore, the reactivity increases with increasing alkene chain length due to an inductive effect (Panyaburapa et al., 2007). As a matter of fact, the electron-donating properties of the alkyl groups enhance the nucleophilicity of double bonds, making them more reactive. To sum up, the reactivity of the olefins in the epoxidation reaction with hydrogen peroxide on TS-1 is mainly determined by two key factors, the inductive effect of the alkyl groups and the solubility of the olefins in methanol.

Fig. 19 suggests an increase in the activity with the length of the olefin carbon chain. This result in comparison with the single olefin compound epoxidation is contradictory (Clerici et Ingallina, 1993). Nevertheless, the solubility of the olefins plays a major role in the differences observed. The profound change in the activity with the TOS for 1-butene epoxidationmight be related to the agglomeration of by-products in the pores of the catalyst . The epoxidation mechanism has been suggested to be of the Eley-Rideal type (Gordon et al., 2020) consisting of an activation step and a reaction step. The activation implies the interaction of hydrogen peroxide and the titanium site for the creation of a hydroperoxo species. This can take place in the entrance region of the pore and inside the pore as has been proposed in literature (Gordon et al., 2020). In the reaction step, the olefin interacts with the hydroperoxo species for the formation of the epoxide molecule and water. The epoxidation process of 1-butene more likely takes place inside the catalyst pores, while, propene and ethene can react easily both inside and outside of the pores. This correlation between the agglomeration of by-products and titanium positions could explain

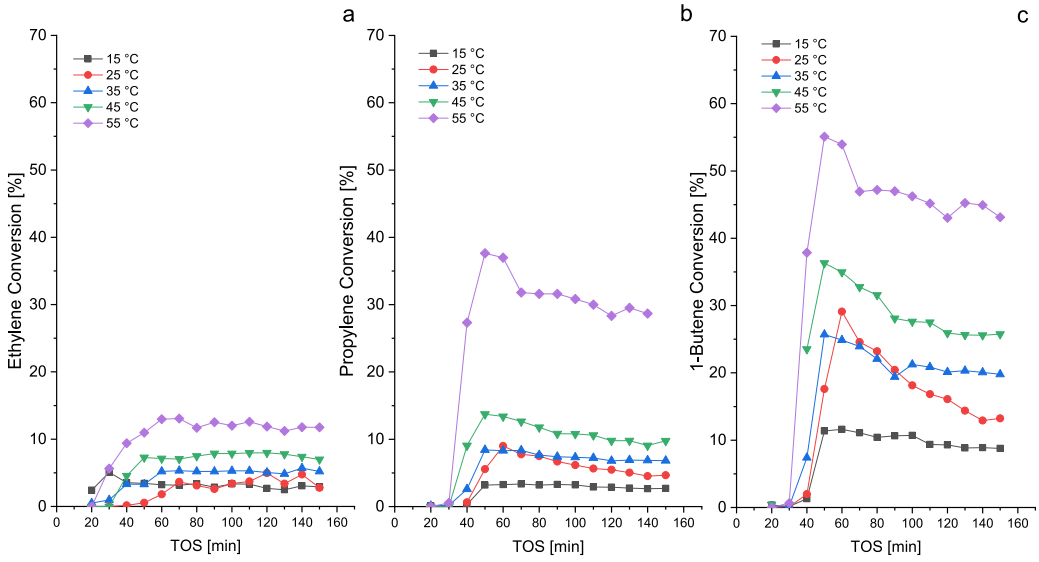

Fig. 12. Effect of reaction temperature on ethene (a), propene (b) and 1-butene (c) conversions. Reaction conditions: P = 1 bar; LFR = 0.5 mL/min; GFR = 0.446 mmol/min; wt% H_2O_2 = 2.

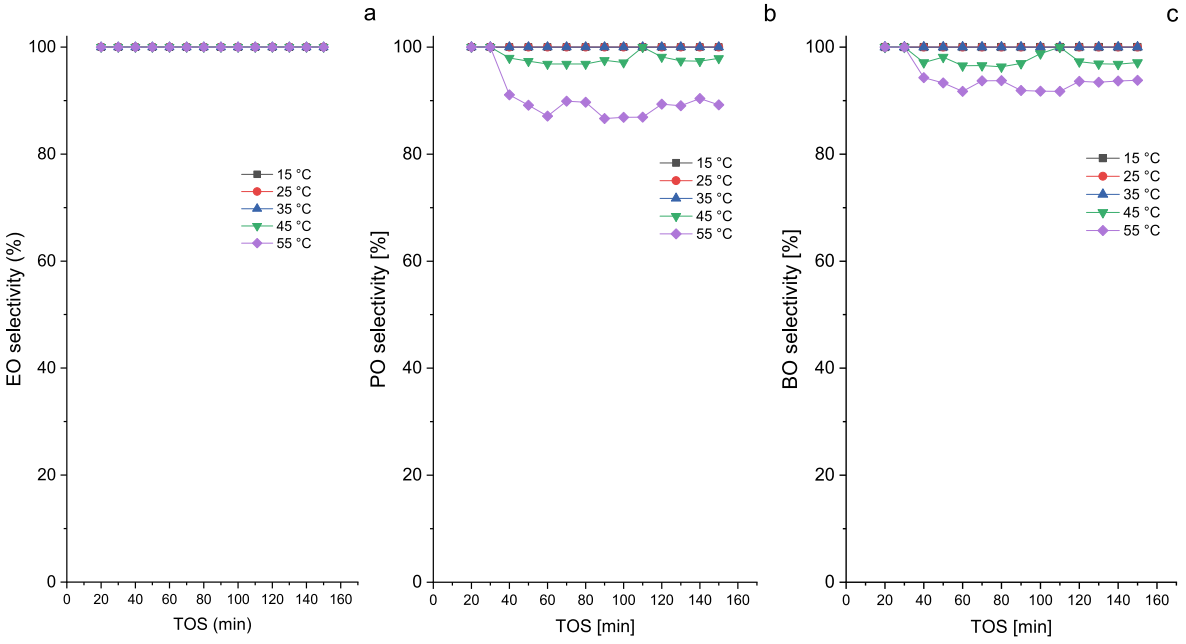

Fig. 13. Effect of reaction temperature on EO (a), PO (b) and BO (c) selectivities. Reaction conditions: P = 1 bar; LFR = 0.5 mL/min; GFR = 0.446 mmol/min; wt% H_2O_2 = 2.

the changes with the time-on-stream for 1-butene epoxidation and the stability of the process for the shorter olefins.

4. Mathematical modelling

4.1. Model assumptions

The mathematical model and parameter estimation procedures for the epoxidation of the ternary olefin mixtures in the presence of the TS-1 catalyst in the trickle bed reactor is presented and discussed. The experimental equipment was the same as reported previously (Alvear et al., 2021a, 2021b) and the catalyst and the flow conditions were similar, too. Therefore, it is reasonable to adopt the same fundamental model hypotheses as reported in our previous work. According to the three-phase dynamic model previously introduced by Alvear et al. (2022), the basic assumptions considered in this modeling effort are listed below.

1. The trickle bed reactor (TBR) is operated isothermally because of moderate reaction enthalpies and the absence of heat transfer limitations.
2. Uniformity of the catalytic bed is assumed.
3. Negligible radial concentration variations are presumed in the bed.
4. Axial dispersion model is chosen to describe the deviations of the flow pattern from ideal plug flow.
5. Internal diffusion limitations in the catalyst particles are neglected, because the reaction was slow and very small catalyst particles were used.

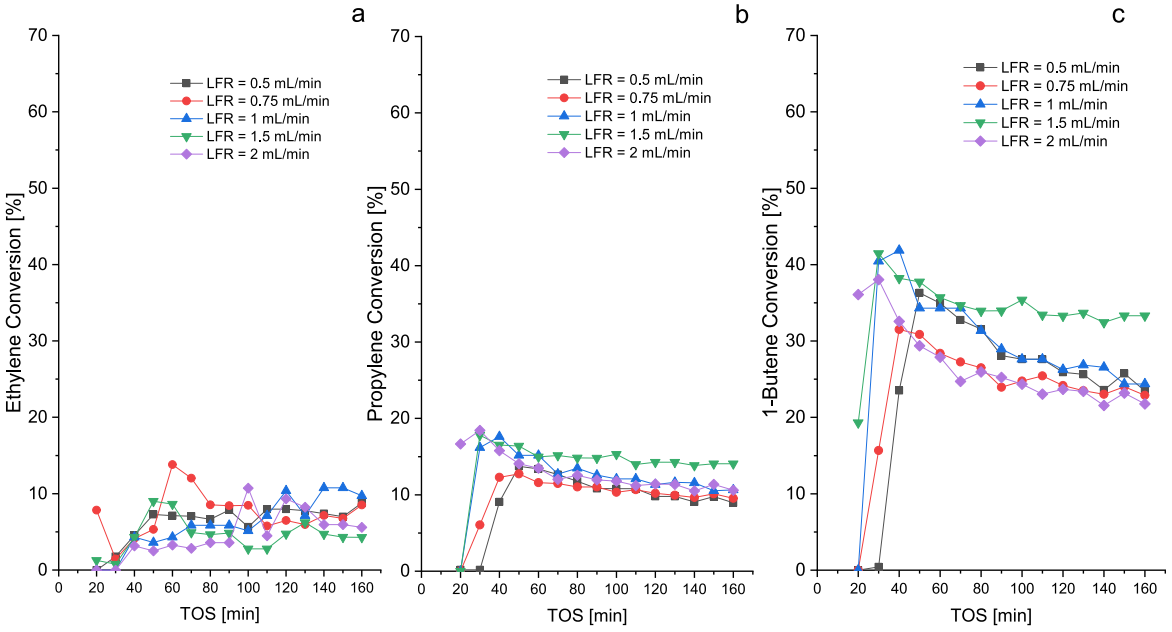

Fig. 14. Effect of LFR on ethene, propene and 1-butene conversions. Reaction conditions: T = 45 °C; P = 1 bar; GFR = 0.446 mmol/min; wt% H_2O_2 = 2.

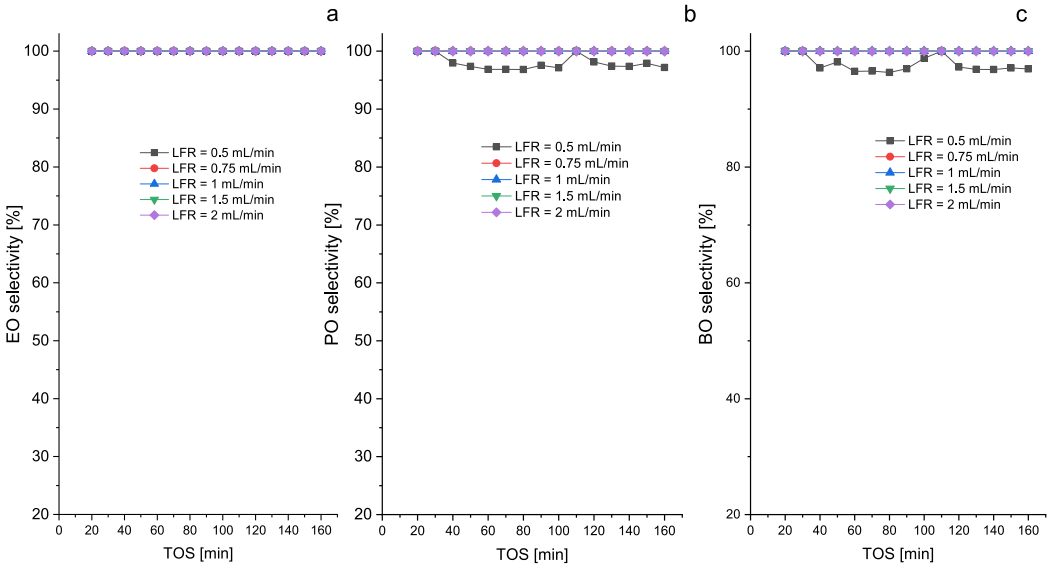

Fig. 15. Effect of LFR on EO, PO and BO selectivities. Reaction conditions: T = 45 °C; P = 1 bar; GFR = 0.446 mmol/min; wt% H_2O_2 = 2.

4.2. Mass balance equations

The dynamic mass balance of each component in the gas phase volume elements is described by equation (1),

$$\varepsilon_G \frac{\partial C_{i,G}}{\partial t} = -\frac{u_G}{L}\frac{\partial C_{i,G}}{\partial \chi} + \frac{\varepsilon_G u_G}{Pe_G L}\frac{\partial^2 C_{i,G}}{\partial \chi^2} - N_{GL} a_{GL} \tag{1}$$

The gas–liquid flux N_{GL} [mol m^{-2} s^{-1}] is defined in equation (2) and it is obtained by assuming negligible the diffusion resistance in the gas film at the gas–liquid interface. Dimensionless Henry's constant H is defined as the ratio between the concentration of compound i at the interface in the gas film and the same in the liquid film.

$$N_{GL} = \frac{C_{i,G} - HC_{i,L}}{H/k_L} \tag{2}$$

The liquid-phase mass balance, the variation in the concentration of the component i over time (t) and dimensionless length coordinate (χ) is given by

$$\varepsilon_L \frac{\partial C_{i,L}}{\partial t} = -\frac{u_L}{L}\frac{\partial C_{i,L}}{\partial \chi} + \frac{\varepsilon_L u_L}{Pe_L L}\frac{\partial^2 C_{i,L}}{\partial \chi^2} + N_{GL} a_{GL} - N_{LS} a_{LS} \tag{3}$$

which gives the concentration profiles of component i over t and χ. As the pseudo-steady state assumption is applied for the outer surface of the catalyst, i.e., the reactants and products do not accumulate on the catalyst outer surface, the liquid–solid flux N_{LS} is coupled to the steady-state reaction kinetics as follows,

$$N_{LS} a_{LS} + \eta_{LS} \rho_B \sum \nu_{i,j} R_j = 0 \tag{4}$$

In trickle bed reactors, the liquid typically flows non-uniformly over the catalyst particles resulting in different degrees of wetting

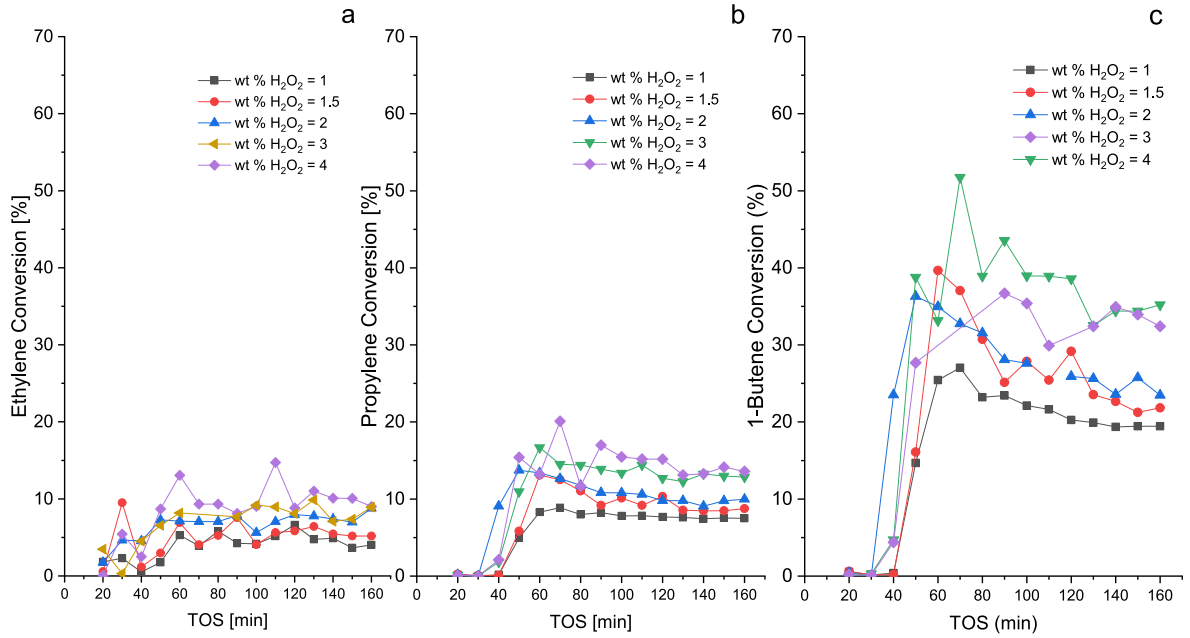

Fig. 16. Effect of H_2O_2 concentration on ethene (a), propene (b) and 1-butene (c) conversions. Reaction conditions: T = 45 °C; P = 1 bar; LFR = 0.5 mL/min; GFR = 0.446 mmol/min.

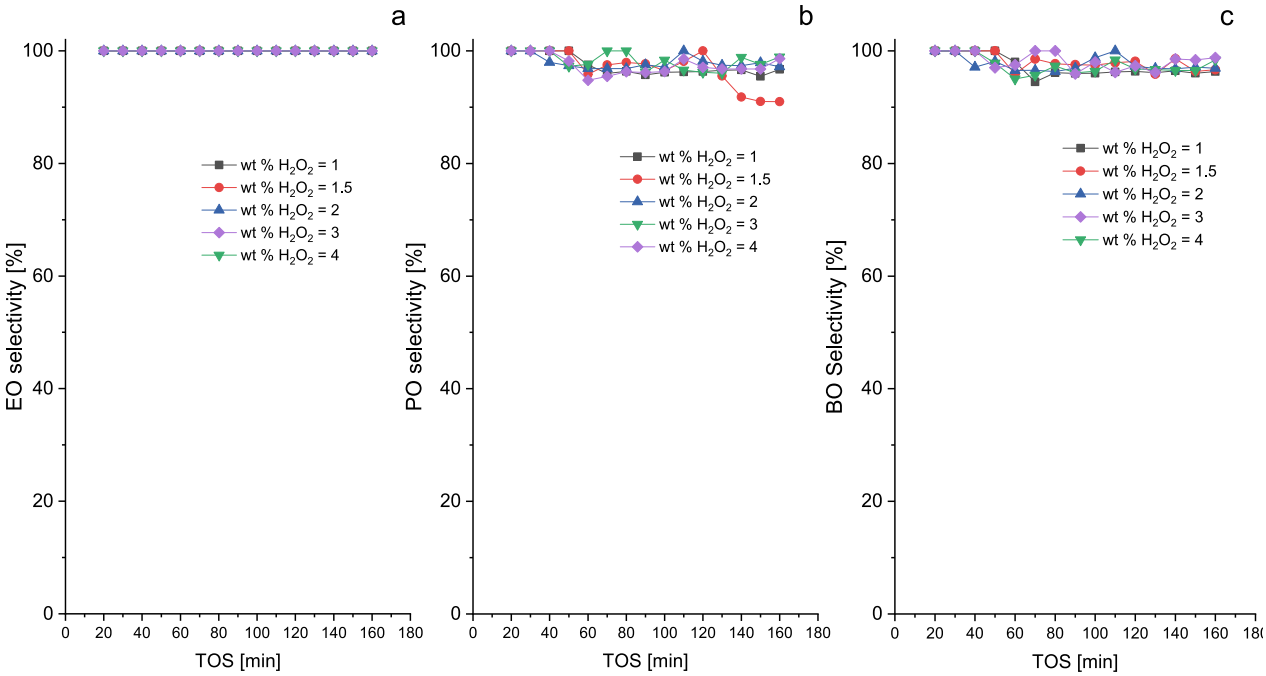

Fig. 17. Effect of H_2O_2 on EO, PO and BO selectivities. Reaction conditions: T = 45 °C; P = 1 bar; GFR = 0.446 mmol/min; wt% H_2O_2 = 2.

(η_{LS}), i.e., complete, partial, or incomplete wetting, which affects the reactor performance (Ranade et al., 2011).

In the actual case, the catalyst particles were considered partially wetted, and a wetting efficiency (η_{LS}) was included in the liquid mass balance

$$\varepsilon_L \frac{\partial C_{i,L}}{\partial t} = -\frac{u_L}{L}\frac{\partial C_{i,L}}{\partial \chi} + \frac{\varepsilon_L u_L}{Pe_L L}\frac{\partial^2 C_{i,L}}{\partial \chi^2} + N_{GL}a_{GL} + \eta_{LS}\rho_B \sum \nu_{ij} R_i \qquad (5)$$

Many correlations for the wetting efficiency in trickle bed reactors have been proposed in scientific literature. Similarly, to Mills and Dudukovic (1981) correlation, a simple power low equation has been suggested to describe the dependence of the wetting efficiency to the liquid flow rate according to equation (6)

$$\eta_{LS} = \alpha Q_L^{\beta} \qquad (6)$$

The exponent β and the multiplication constant α were both obtained by parameter estimation from experimental data. To solve the parabolic partial differential equations (PDEs) (1) and (5), the boundary (BC) and initial conditions (IC) should be selected carefully. The BCs are defined as follows,

$$C_{i,k}\big|_{\chi=0} = C_{i,k,feed} \quad k = G, L \qquad (7)$$

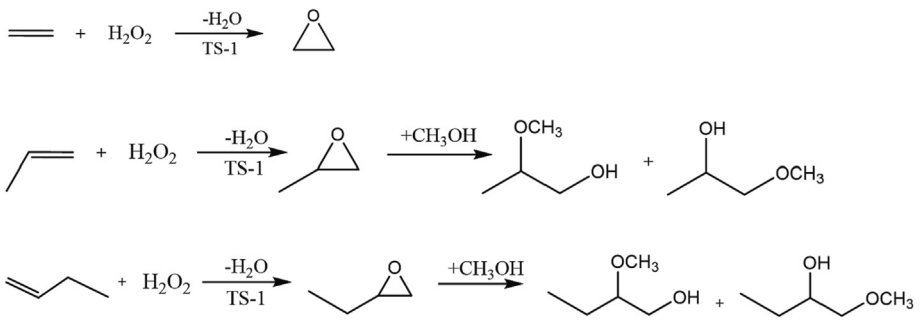

Fig. 18. Reaction scheme.

Table 3
Comparison between calculated Henry's constants with MSRK equation and found in literature at 25 °C and 1 atm (Sahgal et al., 1978; Miyano and Fukuchi, 2004; Miyano et al., 2003).

	H calculated MPa	*H* from literature MPa	Deviation MPa
Ethene	32	27.5	−4.5
Propene	7.2	6.9	−0.3
1-Butene	3.1	2.6	−0.5

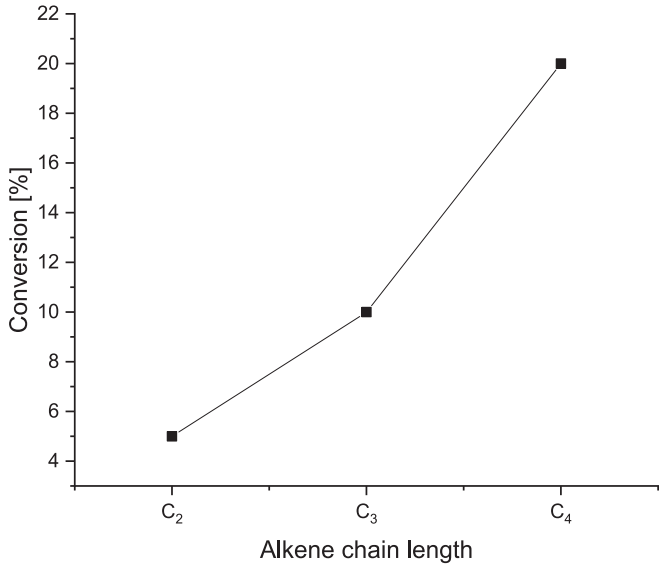

Fig. 19. Effect of alkene chain length on olefin conversion.

$$\left.\frac{\partial C_{i,k}}{\partial \chi}\right|_{\chi=1} = 0 \quad k = G, L \tag{8}$$

The boundary condition (7) is an approximation of the closed inlet boundary condition of Danckwerts (1953), because the Péclet number was high. The Péclet number for the liquid phase (Pe_L) and the liquid hold-up (ε_L) were estimated by fluid dynamics experiments conducted in our previous work (Alvear et al., 2022). The initial conditions are defined by equations (9) and (10). As the reactor is pre-saturated with the gas phase at t = 0, the initial concentration of the olefin i in the gas phase is equal to the feed concentration. A similar assumption was made for the liquid phase.

$$C_{i,G}(t=0) = C_{i,G,feed} \tag{9}$$

$$C_{i,L}(t=0) = C_{i,L,feed} \tag{10}$$

For the gas phase, plug-flow behavior was assumed (Pe_G = 1000) and the gas hold-up was calculated from

$$\varepsilon_G = 1 - \varepsilon_L - \varepsilon_S \tag{11}$$

4.3. Physical properties and correlations

Thanks to its extensive library of chemical components and data, CHEMCAD v.7.1.5 software was utilized to calculate the chemical and physical parameters of the liquid phase, i.e., density (ρ_L), viscosity (μ_L) and surface tension (σ_L) under different operation conditions. The gas phase was considered to be ideal in the investigated range of temperature and pressure (15–55 °C and 1 bar). Therefore, the ideal gas law was used to calculate the gas phase density (ρ_G) and the molar fractions of alkenes, water and methanol. The impact of H_2O_2 on the gas-phase composition was negligible, whereas the influence of methanol and water was temperature dependent, according to the calculations based on vapor pressure data. Once all the parameters had been estimated, the flow regime was confirmed by the aid of an empirical flow map. As expected, a low interaction, the trickle flow regime was found to prevail under the experimental conditions studied (Alvear et al., 2021a, 2021b; Dudukovic et al., 2013; Ranade et al., 2011; Gunjal et al., 2005). Throughout the years, various correlations for gas–liquid mass transfer coefficients in trickle beds have been developed, depending on different parameters and flow regimes. As the correlation proposed by Wild et al. (1992) is valid for the low interaction regime, it was used to calculate the gas–liquid mass transfer coefficients, expressed as the merged parameter k_L-a_L [min^{-1}],

$$\frac{k_L a_L d_k^2}{D_{i,L}} = 2.8 \times 10^{-4} \left[X_G^{1/4} Re_L^{1/5} We_L^{1/5} Sc_L^{1/2} \left(\frac{a_v d_k}{1-\varepsilon_B} \right)^{1/4} \right]^{3.4} \tag{12}$$

According to the correlation of Wild et al. (1992), the mass transfer coefficient is a function of the Lockhardt-Martinelli ratio (X_G), the Reynolds (Re_L), Weber (We_L) and Schmidt (Sc_L) numbers, as well as of the Krischer-Kast hydraulic diameter (d_k) and the diffusivity of the olefin in methanol ($D_{i,L}$), calculated by the Wilke-Chang equation (Wilke and Chang, 1955; Wild and Charpentier, 1987) (in cm^2/s),

$$D_{A,B} = \frac{7.4 \times 10^{-8} (\phi M_B)^{0.5} T}{\mu_B V_A^{0.6}} \tag{13}$$

The parameters appearing in the expression are the association factor of the solvent (ϕ = 1.9 for methanol), the molecular weight of the solvent B (M_B), the temperature (T), the solvent viscosity (μ_B) and the molar volume of the solute A at its normal boiling point (V_A), calculated with the Le Bas method based on atomic increments (Reid et al., 1988). The molecular diffusivities of ethene, propene and 1-butene (A) in methanol (B) at 45 °C were estimated to $4.53 \cdot 10^{-9}$, $3.55 \cdot 10^{-9}$ and $2.99 \cdot 10^{-9}$ $m^2\ s^{-1}$, respectively.

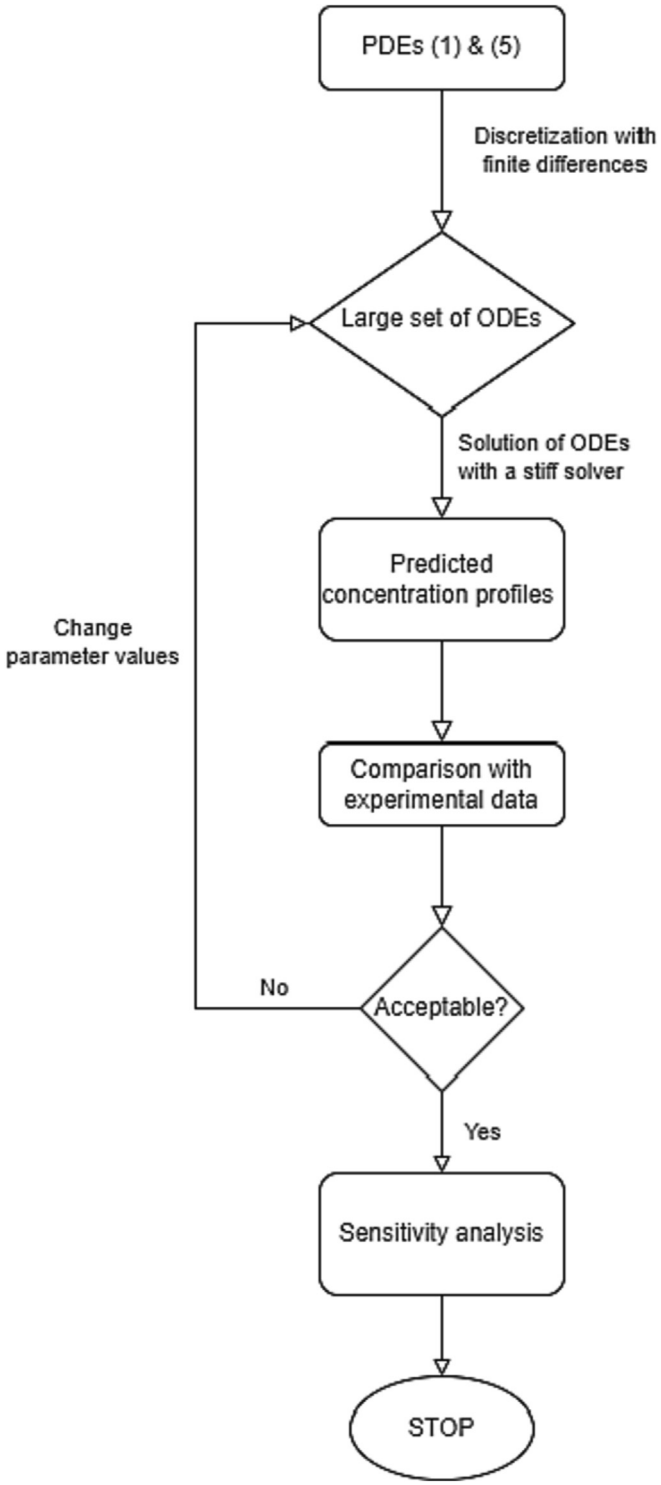

Fig. 20. Flowsheet of the numerical procedures.

As the epoxidation of ethene, propene and 1-butene proceeds in the H_2O_2/MetOH liquid phase, the solubility of the three gases in this solution was calculated. The amount of a gas dissolved in a liquid is described by Henry's law, valid for diluted systems. CHEMCAD v.7.2.5 software was used to estimate the solubility constants (H) of the olefins in the liquid phase at 15–55 °C. The Modified Soave-Redlich-Kwong (MSRK) equation of state was used to predict the vapor–liquid equilibria and it revealed a good accordance with literature values (Table 3). The estimated Henry's constants showed a linear behavior with respect to temperature. The linear plots are are shown in Supporting material.

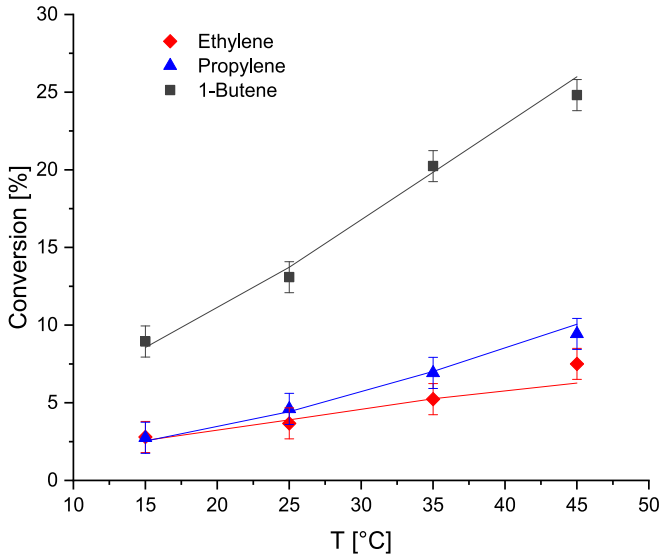

Fig. 21. Effect of reaction temperature on ethene, propene and 1-butene steady-state conversions.

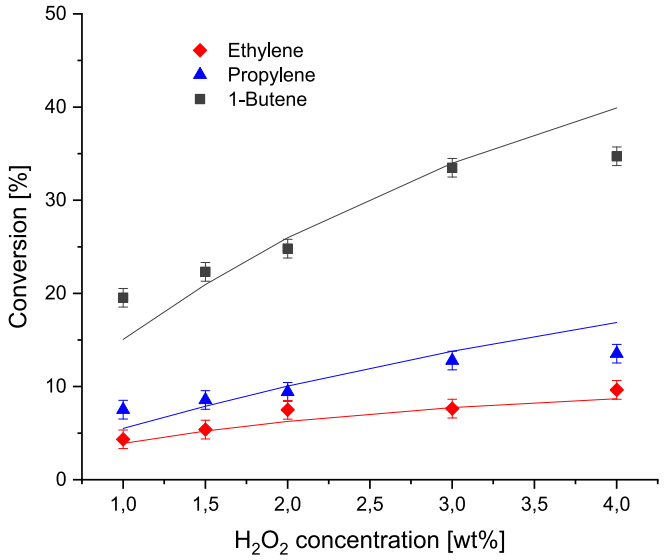

Fig. 22. Effect of hydrogen peroxide concentration on ethene, propene and 1-butene steady-state conversions.

4.4. Kinetic equations for ternary mixture epoxidation

The steps for the epoxidation of ethene-propene-1-butene mixture with hydrogen peroxide promoted by TS-1 can be briefly described as follows. The olefins diffuse from the gas to the liquid phase and react with hydrogen peroxide to produce ethene oxide (EO), propene oxide (PO) and 1-butene oxide (BO), after which they can react further with methanol in the ring opening reactions. However, only single epoxidation reactions are considered here because the selectivities to epoxides always exceeded 90 %. A simplified set of elementary steps can be described as follows (* active $T(OSi)_4$ site on TS-1, A_j = alkene, E_j = epoxide),

$H_2O_2 + * = H_2O_2{}^*$ (I)

$H_2O_2{}^* + A_j \rightarrow H_2O + E_j{}^*$ (II)

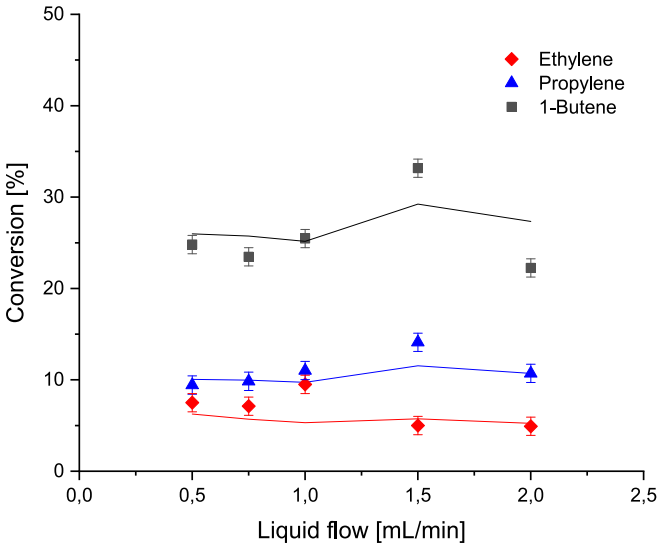

Fig. 23. Effect of the liquid flow rate on ethene, propene and 1-butene steady-state conversions.

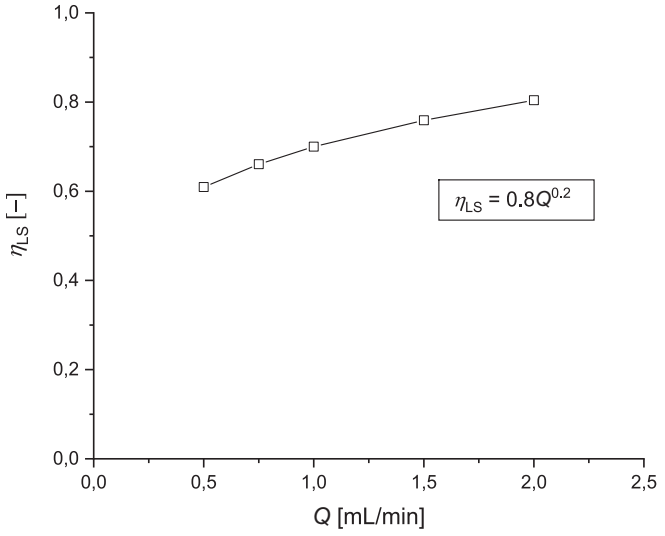

Fig. 24. Predicted wetting efficiency as a function of liquid flowrate.

Table 4
Parameter estimation results of ethene-propene-1-butene mixture epoxidation. The reference kinetic constants are calculated at 318 K.

Kinetic Parameter	Value	Confidence Interval 95 %
Ea_1 [kJ mol^{-1}]	52	16
Ea_2 [kJ mol^{-1}]	50	9
Ea_3 [kJ mol^{-1}]	43	3
$k_{0,1}$ [m^3 mol^{-1} min^{-1}]	6.0 × 10^{-6}	1.0 × 10^{-6}
$k_{0,2}$ [m^3 mol^{-1} min^{-1}]	3.0 × 10^{-6}	0.2 × 10^{-6}
$k_{0,3}$ [m^3 mol^{-1} min^{-1}]	4.7 × 10^{-6}	0.2 × 10^{-6}
α [min^{-1} mL]	0.7	0.1
β [-]	0.2	0.1

$A_j^* = E_j + *$ (III)

$H_2O_2 + A_j \rightarrow H_2O + E_j$

After assuming that the surface reaction step (II) is rate limiting, whereas the adsorption and desorption steps (I) and (III) are rapid compared to the surface reaction, the quasi-equilibrium hypothesis can be applied to the adsorption and desorption steps. Furthermore, the total balance of the surface species is valid; the total concentration of surface sites is denoted by c_0. This reasoning gives the steady-state rate equation (14) for epoxidation. The details are reported in Supporting material.

$$R_j = \frac{k_j' K_{H2O2} C_{Aj} C_{H2O2} C_0}{1 + \sum K_{Ej} C_{Ej} + K_{H2O2} C_{H2O2}} \tag{14}$$

In equation (14) j refers to ethene, propene and 1-butene and to the corresponding epoxides. In the nominator, the product of the parameters $k_j' K_{H2O2} C_0$ can be merged to a single adjustable parameter k_j. Furthermore, the adsorption constants of the molecules on the catalyst are approximated to be negligible as the liquid phase was very diluted. Therefore, the Eley-Rideal rate equations are compressed to power-law kinetics since the denominators in the original rate expressions are reduced to unity: $(1 + K_{H2O2} C_{H2O2} + \sum K_j C_{Ej}) \approx 1$. Consequently, the reaction rates were described with the following equations,

$$R_1 = k_1 C_{H_2O_2} C_{C_2H_4} \tag{15}$$

$$R_2 = k_2 C_{H_2O_2} C_{C_3H_6} \tag{16}$$

$$R_3 = k_3 C_{H_2O_2} C_{C_4H_8} \tag{17}$$

The kinetic constant of the j-th reaction, k_j depends on the reaction temperature by a modified Arrhenius law,

$$k_j = k_{0,j} \left[\exp\left(-\frac{Ea_j}{R} \left(\frac{1}{T} - \frac{1}{T_{ref}} \right) \right) \right] \tag{18}$$

where $k_{0,j}$ is the reference kinetic constant calculated at a reference temperature T_{ref}, Ea is the activation energy and R is the gas constant. The modified form of the Arrhenius law was used to suppress the mutual correlation between the pre-exponential factor and the activation energy.

4.5. Numerical strategies

The partial differential equations (PDEs) (1) and (5) describing the trickle bed model were solved by gPROMS ModelBuilder v.4.0.0 software52 applying the method of lines (MOL) algorithm (Process Systems Enterprise, 2004). MOL transforms PDEs to a system of ordinary differential equations (ODEs) by replacing the spatial derivatives with discretization with finite differences. In this way, the time remains the only independent variable in the system. Various methods of discretization can be used such as centered, backward or forward finite difference methods. In this case, the backward finite difference method (BFDM) of first order was employed as the discretization method for the first derivatives (the plug flow term), whereas the central difference method was applied for the axial dispersion term. The number of discretization points was equal to 30 in the computations. The maximum likelihood estimation method (MAXLKHD) included in gPROMS software was applied for the parameter estimation to obtain the best possible values of the adjustable parameters. The determination of the unknown parameters was performed by maximizing a likelihood function which searches for the parameter values that describe the data with the highest probability. A flowsheet of the numerical procedures is provided in Fig. 20.

5. Modelling results and discussion

5.1. Effect of temperature

The reaction temperature was varied from 15 to 55 °C with an increasing step of 10 °C. The ethene, propene and 1-butene conversions were improved by increasing the reaction temperature, as shown in Fig. 21. For irreversible reactions, like in this case, the

Table 5
Correlation matrix of the estimated parameters.

	Ea_1	Ea_2	Ea_3	$k_{0,1}$	$k_{0,2}$	$k_{0,3}$	α	β
Ea_1	1							
Ea_2	0.02	1						
Ea_3	0.05	0.05	1					
$k_{0,1}$	0.40	−0.01	−0.02	1				
$k_{0,2}$	−0.01	0.10	−0.07	0.20	1			
$k_{0,3}$	−0.01	−0.04	0.02	0.20	0.60	1		
α	−0.03	−0.05	−0.10	−0.01	0.01	−0.01	1	
β	−0.01	−0.01	−0.02	−0.20	−0.40	−0.60	0.80	1

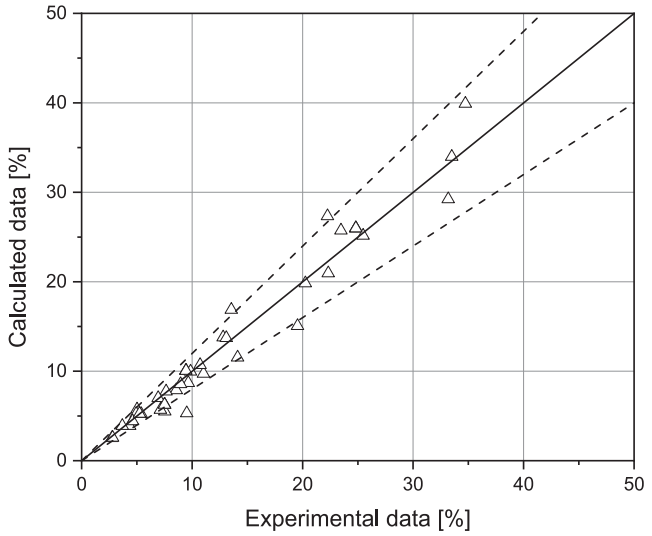

Fig. 25. Parity plot of experimental and predicted data.

temperature affects the kinetics only but not the thermodynamics, resulting in the enhancement of the intrinsic reaction rate with temperature.

5.2. Effect of hydrogen peroxide concentration

The weight fraction of hydrogen peroxide was varied to study its effect on ethene, propene and 1-butene conversion as well as on the epoxide selectivity. As shown in Fig. 22, the conversions increased by concentrating the liquid phase from 1 to 3 wt% of hydrogen peroxide in methanol. At higher concentrations, the hydrogen peroxide decomposition becomes relevant as well as its adsorption on the catalyst surface, decreasing available catalytic sites for olefin adsorption. The conversions of ethene and propene are quite well predicted by the model, but the 1-butene predicted 1-butene conversion had a higher deviation from the experiments. This is due to the model simplification, i.e. neglecting the adsorption parameter of hydrogen peroxide in the rate equations (14)–(16).

5.3. Effect of liquid flow rate

The ternary mixture showed a considerably complex behavior as the liquid flow rate was increased from 0.5 to 2 mL/min. Although a reduction of the residence time was expected to negatively affect the olefin conversions, they did not remarkably change as shown in Fig. 23. In addition, the propene and 1-butene conversions showed a maximum at 1.5 mL/min, while the ethene conversion had a maximum at 1 mL/min. A competition between two effects needs to be considered: optimization of residence time and mass transfer. Until 1.5 mL/min, the reduction in the residence time is balanced by the increase of the mass transfer coefficient k_L-a_L, which depends on the liquid flow rate (Wild et al., 1992). At higher liquid flow rates, the mass transfer rate is high, but the residence time effect is predominant reducing the olefin conversion. The predicted wetting efficiency is displayed in Fig. 24.

5.4. Parameter estimation statistics

The parameter estimation results of the ternary mixtures are presented here. The activation energies (Ea), kinetic constants at the reference temperature (k_0) as well as the wetting efficiency parameters (α and β from Eq. (6)) estimated by nonlinear regression analysis are listed in Table 4. The 95 % confidence intervals of the parameters are reported in the table.

The activation energies obtained are within the common range values for catalytic processes (30–200 kJ mol^{-1}). As shown in Table 4, the sensitivity of the reaction rate with temperature decreases with an increasing olefin chain length from ethene to 1-butene. The exponent β of the liquid flow (Eq. (6)) resulted to be equal to 0.2, which is in agreement with the information found in literature (Mills and Dudukovic, 1981). The correlation matrix representing the statistical relationship between two parameters is reported in Table 5. Most of the correlation coefficients in the matrix are less than 0.4, which is a very satisfactory result. The parity plot displayed in Fig. 25 confirms the normal distribution of the residuals withinin the range ± 20 %.

6. Conclusions

This work demonstrated the possibility to epoxidize mixtures of ethene, propene and 1-butene, using hydrogen peroxide as the oxidant and TS-1 as the heterogeneous catalyst. The transient behavior of the step responses of the alkenes and epoxides revealed following phenomena: the alkenes are epoxidized simultaneously, and the dynamics is enhanced by increasing temperature and hydrogen peroxide concentration. The epoxide selectivities were stable and high after an induction period, exceeding in most cases 90 %. The highest conversions of alkenes was obtained for 1-butene, which can be explained by its highest solubility among the alkenes studied.

A laboratory-scale trickle bed reactor was employed in all the experiments and it was described mathematically by a heterogeneous axial dispersion model involving rate equations as well as mass transfer and dispersion effects. Parameter estimation with nonlinear regression analysis allowed to obtain numerical values of the kinetic constants at reference temperature, as well as activation energies and liquid–solid mass transfer parameters. The model gave a reasonable agreement with steady-state experimental data.

A significant process intensification might be applied by direct epoxidation of olefin mixtures with TS-1 and hydrogen peroxide, being both economically and environmentally beneficial. As a matter of fact, separation steps would be drastically reduced and mild

operating conditions of temperature and pressure would be employed, still reaching high epoxide selectivities and alkene conversions. Moreover, bio-based α-alkenes produced by a combined reverse water–gas shift reaction and Fischer-Tropsch process for alkene production might be used for the epoxidation process. In this way, the more traditional oil-based olefins can be replaced by more sustainable alternatives.

CRediT authorship contribution statement

Matias Alvear: Conceptualization, Methodology, Formal analysis, Software, Writing – original draft, Writing – review & editing, Supervision. **Federica Orabona:** Methodology, Formal analysis, Software, Writing – original draft. **Kari Eränen:** Conceptualization, Methodology, Resources, Project administration, Funding acquisition, Supervision. **Juha Lehtonen:** Conceptualization, Methodology, Resources, Project administration, Funding acquisition, Supervision. **Sari Rautiainen:** Conceptualization, Methodology, Supervision. **Martino Di Serio:** Conceptualization, Methodology, Writing – review & editing, Resources, Project administration, Funding acquisition, Supervision. **Vincenzo Russo:** Conceptualization, Methodology, Formal analysis, Writing – original draft, Writing – review & editing, Resources, Project administration, Funding acquisition, Supervision. **Tapio Salmi:** Conceptualization, Methodology, Formal analysis, Writing – original draft, Writing – review & editing, Resources, Project administration, Funding acquisition, Supervision.

Data availability

Data will be made available on request.

Declaration of Competing Interest

The authors declare that they have no known competing financial interests or personal relationships that could have appeared to influence the work reported in this paper.

Acknowledgement

This work is part of the activities financed by Academy of Finland, through the Academy Professor grants 319002, 320115, 345053 (T. Salmi, M. Alvear). The BECCU research project coordinated by VTT Technical Research Centre of Finland Ltd with main funding from Business Finland is gratefully acknowledged (F. Orabona).

Appendix A. Supplementary material

Supplementary data to this article can be found online at https://doi.org/10.1016/j.ces.2023.118467.

References

Alvear, M., Eränen, K., Murzin, D., Salmi, T., 2021a. A study of the product distribution in the epoxidation of propylene over TS-1 catalyst in a trickle bed reactor. Ind. Eng. Chem. Res. 60, 2430–2438.
Alvear, M., Fortunato, M.E., Russo, V., Eränen, K., Di Serio, M., Lehtonen, J., Rautiainen, S., Murzin, D., Salmi, T., 2021b. Continuous liquid phase epoxidation of ethylene with hydrogen peroxide on a titanium-silicate catalyst. Ind. Eng. Chem. Res. 60, 9429–9436.
Alvear, M., Fortunato, M.E., Russo, V., Salmi, T., Di Serio, M., 2022. Modelling of transient kinetics in trickle bed reactors: ethylene oxide production via hydrogen peroxide. Chem. Eng. Sci. 2022, (248) 117156.
Berndt, T., Bräsel, S., 2009. Epoxidation of a series of C2–C6 olefins in the gas phase. Chem. Eng. Technol. 32, 1189–1194.
Clerici, M., 2015. The activity of titanium silicalite-1 (TS-1): some considerations on its origin. Kinet. Catal. 56, 450–455.
Clerici, M., Bellussi, G., Romano, U., 1991. Synthesis of propylene oxide from propylene and hydrogen peroxide catalyzed by titanium silicalite. J. Catal. 129, 159–167.
Clerici, M., Ingallina, P., 1993. Epoxidation of lower olefins with hydrogen peroxide and titanium silicalite. J. Catal. 140, 71–83.
Danckwerts, P.V., 1953. Continuous flow systems. Distribution of residence times. Chem. Eng. Sci. 2, 1–18.
Dudukovic, M.P., Kuzeljevic, Z.V., Combest, D.P., 2013. Three Phase Trickle Bed Reactors - Ullmann's Encyclopedia of Industrial Chemistry. Wiley, New York.
Gordon, C.P., Engler, H., Tragi, A.S., Plodinec, M., Lunkenbein, T., Berkessel, A., Teles, J.H., Parvulescu, A.-N., Coperet, C., 2020. Efficient epoxidation over dinuclear sites in titatinium silicalite-1. Nature 586, 708–713.
Grigoropoulou, G., Clark, J.H., Elings, J.A., 2003. Recent developments on the epoxidation of alkenes using hydrogen peroxide as an oxidant. Green Chem. 5, 1–7.
Gunjal, P.R., Kashid, M.N., Ranade, V.V., Chaudhuri, V.R., 2005. Hydrodynamics of trickle bed reactors: experiments and CFD modeling. Ind. Eng. Chem. Res. 44, 6278–6294.
Jess, A., Wasserscheid, P., 2013. Chemical Technology – An Integral Textbook. Wiley, Germany.
Lefort, T.E., 1935. Process for the production of ethylene oxide. US 1998878A. Société Francaise de Catalyse Generalisée.
Mills, P.L., Dudukovic, M.P., 1981. Evaluation of Liquid-solid contacting in trickle-bed reactors by tracer methods. AIChE J. 27, 893–904.
Miyano, Y., Fukuchi, K., 2004. Henry's constants of propane, propene, trans-2-butene and 1,3-butadiene in methanol at 255–320 K. Fluid Phase Equilib. 2, 223–238.
Miyano, Y., Nakanishi, K., Fukuchi, K., 2003. Henry's constants of butane, isobutane, 1-butene and isobutene in methanol at 255–320 K. Fluid Phase Equilib. 208, 223–238.
Notari, B., 1996. Microporous crystalline titanium silicates. Adv. Catal. 41, 253–327.
Panyaburapa, W., Nanok, T., Limtrakul, J., 2007. Epoxidation reaction of unsaturated hydrocarbons with H2O2 over defect TS-1 – investigated by ONIOM method: formation of active sites and reaction mechanisms. J. Phys. Chem. 111, 3433–3441.
Process Systems Enterprise, 2004. gPROMS v3.7.1 User Guide. Process Systems Enterprise Ltd., London.
Ranade, V.V., Chaudhari, R.V., Gunjal, P., 2011. Trickle Bed Reactors – Reactor Engineering and Applications. Elsevier, Netherlands.
Rebsdat, S., Mayer, D., 2000. Ullmann's Encyclopedia of Industrial Chemistry, Vol. 13. Wiley, Germany.
Reid, R.C., Prausnitz, J.M., Poling, B.E., 1988. The Properties of Gases and Liquids. McGraw-Hill, New York.
Russo, V., Tesser, R., Santacesaria, E., Di Serio, M., 2013. Chemical and technical aspects of propene oxide production via hydrogen peroxide (HPPO process). Ind. Eng. Chem. Res. 52, 1168–1178.
Sahgal, A., La, H.M., Hayduk, W., 1978. Solubility of ethylene in several polar and non-polar solvents. Can. J. Chem. Eng. 56, 354–357.
Salmi, T., Mikkola, J.-P., Wärnå, J., 2019. Chemical Reaction Engineering and Reactor Technology, 2nd edition, CRC Press Taylor & Francis Group, Boca Raton, FL, Chapter 6.
Smith, J.G., 1984. Synthetically useful reactions of epoxides. Synthesis 8, 629–656.
Speight, J.G., 2011. Handbook of Industrial Hydrocarbon Processes. Elsevier, Netherlands.
Taramasso, M., Perego, G., Notari, B., 1983. Preparation of porous crystalline synthetic material comprised of silicon and titanium oxides. US 4410501. Snamprogetti S.p.A..
Wild, G., Charpentier, J.-G., 1987. Diffusivité des gaz dans les liquides. Techniques d'ingenieur, Paris 615, 1–13.
Wild, G., Larachi, F., Charpentier, J.C, 1992. Heat and mass transfer in gas-liquid-solid fixed bed reactors. In: Quintard, M., Todorovic, M. (Eds.), Heat and Mass Transfer in Porous Media. Elsevier, pp. 616.
Wilke, C.R., Chang, P., 1955. Correlations of diffusion coefficients in dilute solutions. AIChE J. 20, 611–615.